ISSN 1028-334X, Doklady Earth Sciences, 2006, Vol. 406, No. 1, pp. 52–55. © Pleiades Publishing, Inc., 2006.
Original Russian Text © Sh.A. Mukhamediev, A.N. Galybin, 2006, published in Doklady Akademii Nauk, 2006, Vol. 406, No. 1, pp. 95–98.

GEOPHYSICS

Where and How Did the Ruptures of December 26, 2004 and March 28, 2005 Earthquakes near Sumatra Originate?

Sh. A. Mukhamediev[1] and A. N. Galybin[2]

Presented by Academician S.A. Fedotov June 27, 2005

Received July 4, 2005

DOI: 10.1134/S1028334X06010132

The earthquakes of December 26, 2004, (magnitude $M_w = 9.3$; epicenter coordinates 3.3° N, 96.0° E; depth $h \approx 30$ km [1, 2]; approximately 300 000 victims due to the tsunami on the Indian Ocean coast) and March 28, 2005, ($M_w = 8.6$; 2.1° N, 97.0° E; $h \approx 30$ km [1, 2]; more than 1000 victims), which occurred in the Sunda Trench west of Sumatra Island, confirm the common opinion that the search for factors controlling the origin of great earthquakes in island arcs is a problem of vital importance in seismology. Over the last decades, the problem has mainly been solved by studying the correlation between the distribution of great earthquakes and various parameters of subduction zones, such as rate and age of interacting plates; geometric, rheological, and temperature characteristics of subduction zones; presence of asperities, characteristics of sediments, fluid regime, and so on (see [3–5] and others). These investigations have not revealed any unambiguous relationships [5].

Here, we consider the stress state (SS) as a key factor affecting the origin of great earthquakes. We examine the Sunda Trench region, where the Indian and Australian plates (hereafter, the Indo-Australia Plate, IAP) submerge under the Eurasia Plate (EAP), which is represented there by the Burma and Sunda peripheral plates (Fig. 1). Unlike plate kinematics, which has been sufficiently well studied in the region (Fig. 1), information on the SS is very limited. Experimental information represented by data on stress regimes and on orientation of horizontal principal stresses T_1 and T_2 ($T_1 < T_2$; compressive stresses are positive) are available in the world database WSM [6]. The data are spatially discrete and do not contain stress magnitudes (Fig. 1). One can only infer for the studied region that the axis of maximal compression T_2 is oriented almost perpendicular to the trench on the EAP side and nearly parallel to it on the IAP side. The stress field was previously modeled (see, for instance, [7]) on the basis of traditional approaches in the theory of elasticity, in which boundary forces were adopted from model estimates of driving forces. Such estimates differ by an order of magnitude, which may result in greater discrepancies even if the calculated and experimental orientations of T_2 coincide [8, 9].

To obtain a more realistic result, we consider the IAP and EAP as elastic plates (generally, with different elastic moduli) and apply a direct approach based on experimental data on orientations of T_2 as the only input information. This approach is described in detail in [9, 10], and its main idea is as follows. The horizontal stress tensor field is completely defined by three functions of the Cartesian coordinates x_1, x_2—the mean stress $P = \frac{1}{2}(T_1 + T_2)$, maximum shear stress $\tau_{\max} = \frac{1}{2}(T_2 - T_1)$, and the angle φ between T_2 and x_1 axes. Based on the general solution of plane problem of elasticity [11], these functions are represented as $P = -2\mathrm{Re}\,\Phi(z)$, $\tau_{\max} e^{-2i\varphi} = \bar{z}\,\Phi'(z) + \Psi(z)$, where $z = x_1 + ix_2$, $\bar{z} = x_1 - ix_2$, and Φ', Ψ are holomorphic functions. The potentials $\Phi'(z)$, $\Psi(z)$ are approximated by polynomials of the nth order of z (different for the IAP and EAP), coefficients of which represent the sought quantities. They are found by solving an overdetermined system of linear algebraic equations obtained by fitting the calculated and experimental angles in points of stress measurements; imposing continuity of the stress vector at n_b collocation points on the trench trajectory; and normalizing the function $\tau_{\max}$.

The problem has been solved for polynomials of different orders n and with different numbers n_b of collocation points. Results of the numerical solution slightly vary with n ($n < 5$) and $n_b < 168$. Figures 1 and 2 present the solution obtained for $n = 4$ and $n_b = 167$. It should

[1] *Schmidt Institute of Physics of the Earth, Russian Academy of Sciences, Bol'shaya Gruzinskaya ul. 10, Moscow, 123995 Russia; e-mail: shamil@ifz.ru*

[2] *Wessex Institute of Technology, Ashurst Lodge, Ashurst, Southampton, SO40 7AA, UK; e-mail: agalybin@wessex.ac.uk*

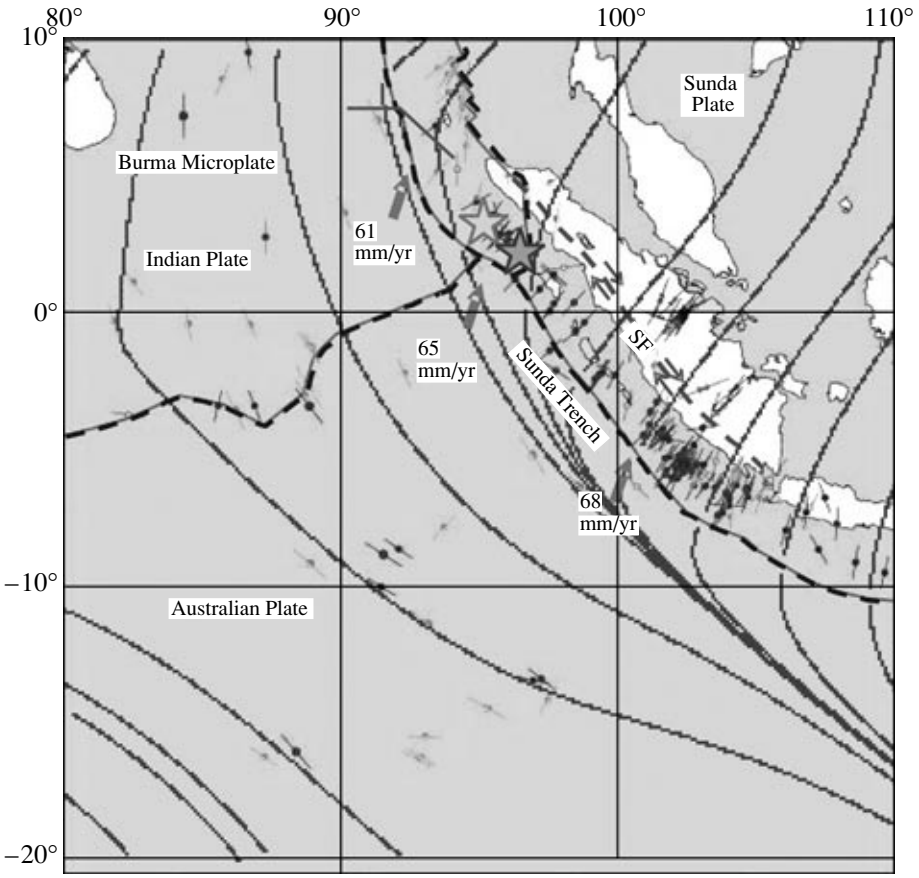

Fig. 1. Kinematics of plate convergence and stress elements in epicenters of the earthquakes of December 26, 2004 (☆) and March 28, 2005 (★); (⎓) plate boundaries; (↗) motion of the IAP relative to EAP [1] with partition in the course of subduction into underthrusting (normal to the Sunda Trench axis) in the seismogenic zone of plate interaction and dextral horizontal strike-slip fault along the Sumatra Fault (SF) [1]; short segments designate the orientation of the axis of maximum compression T_2 [6]; (—) calculated trajectories of T_2.

be noted that the function φ and, hence, the trajectories of principal stresses are determined uniquely, and the fields of τ_{max} and P are expressed to the accuracy of linear transformations as $\tau_{max} \to a\tau_{max}$, $P \to aP + b$, where a ($a > 0$) and b are arbitrary constants. The field of the complete stress tensor **T** is found by superposition of the obtained solution and the lithostatic stress varying with depth due to the rock weight and horizontal stress. The procedure does not affect the horizontal fields of trajectories or τ_{max}.

Let us emphasize the following distinctive features of the stress field:

in the vicinity of the trench, trajectories T_2 are subnormal and, hence, trajectories T_1 are shear to its strike (Fig. 1);

τ_{max} is low in an elongated area extending along the trench and crossing it near the epicenters of the earthquakes of December 26, 2004 and March 28, 2005 (Fig. 2);

mean stress P for the island arc (northeast of the trench) is lower than the corresponding characteristic value for the IAP (Fig. 2); and

τ_{max} and P reach minimum near epicenters of December 26, 2004 and March 28, 2005 earthquakes (Fig. 2) along the trench (on both EAP and IAP sides), with τ_{max} being continuous across the trench.

Distinctive features of the stress field allow us to investigate the mechanics of initiation of December 26, 2004 and March 28, 2005 earthquakes. Their epicenters are confined to a less stressed area, characterized by lower T_1 and T_2 values (on both the EAP and IAP sides); i.e., the initiation of earthquakes is affected not only by stress T_2 normal to the trench strike, but also by the shear stress T_1. If the inclined seismogenic surface S_i of interaction between the obducting and subducting plates were smooth, then stress T_1, parallel to this surface, would exert no influence on the stresses affecting S_i. Hence, asperities of the surface S_i, which are extending parallel and perpendicular to the S_i strike, play a crucial role in the initiation of earthquake breakups. Such asper-

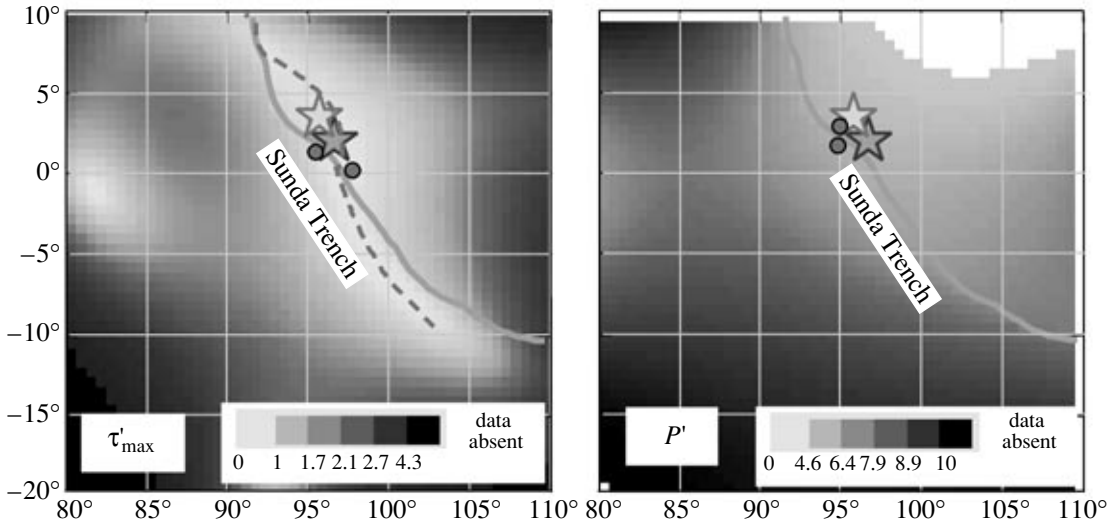

Fig. 2. Relative shear stress τ'_{max} and mean horizontal P' stresses ($\tau_{max} = a\tau'_{max}$, $P = aP' + b$, a = const, $a > 0$, b = const) in epicenters of the earthquakes of December 26, 2004 (☆) and March 28, 2005 (★). Circles denote positions of minimum τ'_{max} and P' values attained when moving along each side of the trench; (---) line of minimum τ'_{max} values attained when moving along a latitude.

ities emerge on the surface S_i due to the subduction of topographic irregularities of the IAP under the EAP.

Figure 3 shows the geometry of surface S_i, coordinate axes and corresponding orts, as well as the orientation of prinicipal stresses T_1 and T_2 relative to S_i. For the sake of simplicity, shear stress T_1 is assumed to be identical for both blocks. Inclination $\vartheta(x_2)$ of surface S_i to the horizon represents a superposition of the generalized slope of the plate and variations of this angle due to the rugged topography of the seabed. Let us denote

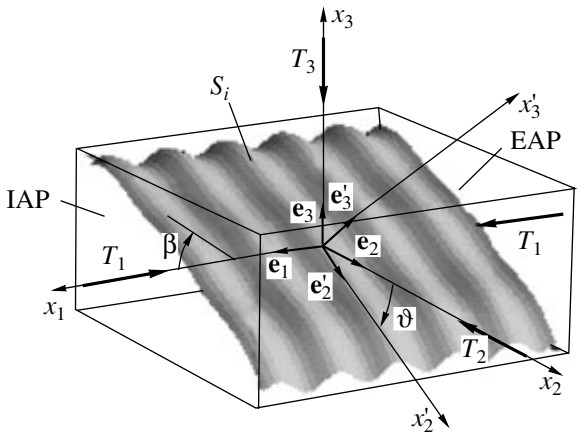

Fig. 3. Geometry of seismogenic surface S_i separating the obducting (EAP) and subducting (IAP) blocks. Axes x_1, x_2 (with orts $\mathbf{e}_1$, $\mathbf{e}_2$) are shear and orthogonal (relative to the trench strike) horizontal axes, respectively. Axes x'_2, x'_3 (with orts $\mathbf{e}'_2$, $\mathbf{e}'_3$) are directed along the S_i surface dip and orthogonal to it, respectively. (↗) principal stress axes.

variations in slope S_i along the trench strike as $\beta(x_1)$. Then the vector $\mathbf{n}$ of the unit normal to S_i, as well as the dimensionless normal stress t_n and the shear stress vector $\mathbf{t}_\tau$, which affect S_i, will be represented as

$$\begin{aligned}
\mathbf{n} &= -\sin\beta\mathbf{e}_1 + \cos\beta(\sin\vartheta\mathbf{e}_2 + \cos\vartheta\mathbf{e}_3),\\
t_n &= \mathbf{n}\cdot\mathbf{T}\cdot\mathbf{n} = \tilde{T}_1 + F\cos^2\beta,\\
\mathbf{t}_\tau &= \mathbf{n}\cdot\mathbf{T} - t_n\mathbf{n} = F\cos\beta\sin\beta(\cos\beta\mathbf{e}_1\\
&+ \sin\beta\mathbf{e}'_3) + (\tilde{T}_2 - 1)\cos\beta\sin\vartheta\cos\vartheta\mathbf{e}'_2, \qquad (1)\\
F &= (\tilde{T}_2 - \tilde{T}_1) - \cos^2\vartheta(\tilde{T}_2 - 1).
\end{aligned}$$

Here $\tilde{T}_i = \dfrac{T_i}{T_3}$, $i = 1, 2$, T_3 is the principal vertical stress.

The Coulomb–Amonton criterion $|\mathbf{t}_\tau| = \mu t_n$ (where μ is the friction coefficient) is satisfied and is accepted further as the condition of the breakage onset. The $\tilde{T}_2$ value is most variable. It increases during a seismic cycle from $\tilde{T}_2 \approx 1$ (in the hypothetical case of a complete shear stress relief along the S_i dip) to a critical value $\tilde{T}_{2(c)}$ realized when the Coulomb–Amonton criterion is satisfied. The relationship between $\tilde{T}_{2(c)}$ and angle ϑ is shown in Fig. 4. For the presented curves, the minimum of $\tilde{T}_{2(c)}$ ($\min\limits_{\vartheta}\tilde{T}_{2(c)}$) is reached within $\vartheta \approx \dfrac{\pi}{6} - \dfrac{\pi}{4}$ range. Asperities with such dip angles will provoke displacement if stress $\tilde{T}_2$ reaches the $\min\limits_{\vartheta}\tilde{T}_{2(c)}$ value. The selected ranges of parameters are as follows: $\mu \approx$

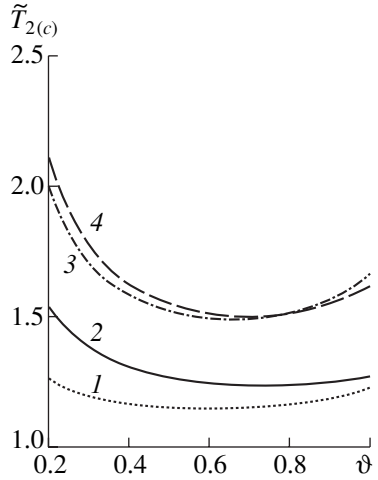

Fig. 4. Variation of critical value $\tilde{T}_{2(c)}$ with slope ϑ of surface S_i at the average value $\langle\beta^2\rangle = 0.05$ and at different values of shear stress $\tilde{T}_1$ and friction coefficient μ. (*1*) $\tilde{T}_1 = 1.5$, $\mu = 0.1$; (*2*) $\tilde{T}_1 = 1.1$, $\mu = 0.1$; (*3*) $\tilde{T}_1 = 1.5$, $\mu = 0.2$; (*4*) $\tilde{T}_1 = 1.1$, $\mu = 0.2$.

0.1–0.2 (that corresponds to estimated μ for some subduction zones [12]) and $\tilde{T}_1 \approx 1.1$–1.5. These ranges provide the condition $\min_{\vartheta}\tilde{T}_{2(c)} > \tilde{T}_1 > 1$ (which is necessary due to the thrust nature of the stress field [6]) and the condition of closeness of $\min_{\vartheta}\tilde{T}_{2(c)}$ and $\tilde{T}_1$ in magnitude. At $\mu > 0.2$, the value $\min_{\vartheta}\tilde{T}_{2(c)}$ substantially exceeds $\tilde{T}_1$; at $\tilde{T}_1 > 1.5$, the condition $\min_{\vartheta}\tilde{T}_{2(c)} > \tilde{T}_1$ is violated. The stress range $\tilde{T}_1 \approx 1.1$–1.5 determined here and the known hypocenter depth ($h \approx 30$ km) allow one to assess the horizontal stress at this depth. At the density $\rho \approx 2.65$ g/cm^3 [13], one obtains $T_1 \approx T_2 \approx (1.1\text{–}1.5)\int_{-h}^{0}\rho\, g\, dx_3 = (9\text{–}12)\cdot 10^2$ MPa.

Thus, the stress field in the IAP–EAP convergence zone has been determined without any assumptions on the magnitudes of driving forces. Based on features of the obtained solution, the mechanism of initiation of the disastrous earthquakes in the Sunda Trench has been proposed. The initial displacement, which provokes an unstable dynamic lateral propagation of the fracture along the subduction surface S_i (for 1200 km during the earthquake of December 26, 2004 [1, 2]), occurs in the area of low values of tectonic stresses owing to a local increase in angle ϑ. The increase takes place due to asperities on S_i, the presence of which is not postulated in our model but is a direct consequence of the calculated stress state. The influence of sediments and temperature and fluid regimes in the subduction zone can be effectively accounted for by decreasing the friction coefficient μ. The model makes it possible to substantially limit variations in horizontal stress (relative to vertical stress) and to estimate absolute values of these stresses at the hypocenter depth.

It should be pointed out that the position of the minimum stress might change following the events of December 26, 2004 and March 28, 2005. Therefore, it is important to monitor the SS to reveal the new position of this minimum stress and take it into account in the tsunami early warning system planned for the Indian Ocean.

ACKNOWLEDGMENTS

This work was partially supported by the Russian Foundation for Basic Research, the Division of Earth Sciences of the Russian Academy of Sciences (Fundamental Program No. 5), and the Australian Computational Earths Systems Simulator (MNRF "ACcESS").

REFERENCES

1. The USGS Web Site http://neic.usgs.gov/neis/bulletin/neic_slav_ts.html. 2005.
2. T. Lay, H. Kanamori, C. J. Ammon, *et al.*, Science **308**, 1127 (2005).
3. M. Cloos, Geology, No. 20, 601 (1992).
4. R. McCaffrey, J. Geophys. Res. **98B**, 11953 (1993).
5. J. F. Pachero, L. R. Sykes, and C. H. Scholz, J. Geophys. Res. **98B**, 14133 (1993).
6. J. Reinecker, O. Heidbach, M. Tingay, *et al.*, www.world-stress-map.org.
7. R. Chose, S. Yoshioka, and K. Oike, Tectonophysics **181**, 223 (1990).
8. Sh. A. Mukhamediev and A. N. Galybin, Fizika Zemli, No. 8, 23 (2001) [Izv. Phys. Solid Earth, **37**, 636 (2001)].
9. Sh. A. Mukhamediev, A. N. Galybin, and B. H. G. Brady, Int. J. Rock Mech. Min. Sci. **43**, 66 (2006). Doi:10.1016.j.ijrmms.2005.04.008.2005.
10. A. N. Galybin and Sh. A. Mukhamediev, Int. J. Solids Struct. **41**, 5125 (2004).
11. N. I. Muskhelishvili, *Some Basic Problems of the Mathematical Theory of Elasticity* (Nauka, Moscow, 1966) [in Russian].
12. K. Wang and J. He, J. Geophys. Res. **104B**, 15191 (1999).
13. M. Simoes, J. P. Avouac, R. Cattin, and P. Henry, J. Geophys. Res. B **109**, 10402 (2004). Doi:10.1029/2003JB002958.